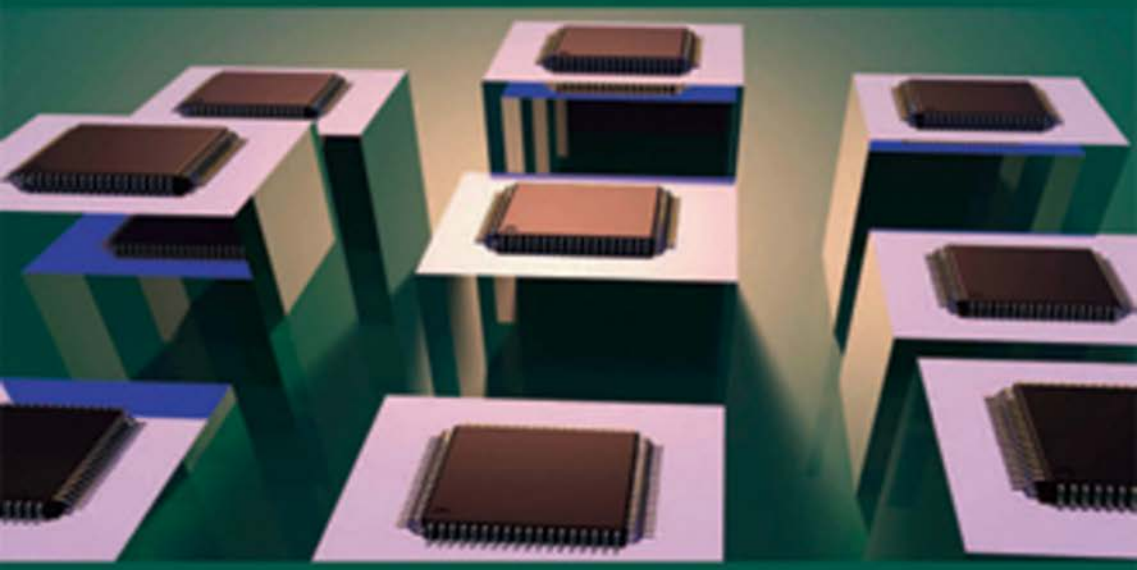

Micro, Nanosystems and Systems on Chips

Modeling, Control and Estimation

Edited by
Alina Voda

iSTE
WILEY

Micro, Nanosystems and Systems on Chips

To Anaïs and Raphaël

Micro, Nanosystems and Systems on Chips

Modeling, Control and Estimation

Edited by
Alina Voda

ISTE

WILEY

First published 2010 in Great Britain and the United States by ISTE Ltd and John Wiley & Sons, Inc.

ISTE Ltd
27-37 St George's Road
London SW19 4EU
UK

www.iste.co.uk

John Wiley & Sons, Inc.
111 River Street
Hoboken, NJ 07030
USA

www.wiley.com

Library of Congress Cataloging-in-Publication Data

Micro, nanosystems, and systems on chips : modeling, control, and estimation / edited by Alina Voda.
p. cm.
Includes bibliographical references and index.
ISBN 978-1-84821-190-2
1. Microelectromechanical systems. 2. Systems on a chip. I. Voda, Alina.
TK7875.M532487 2010
621.381--dc22

2009041386

British Library Cataloguing-in-Publication Data
A CIP record for this book is available from the British Library
ISBN 978-1-84821-190-2

Printed and bound in Great Britain by CPI Antony Rowe, Chippenham and Eastbourne

Contents

Introduction

Micro and nanosystems represent a major scientific and technological challenge, with actual and potential applications in almost all fields of human activity. From the first physics and philosophical concepts of atoms, developed by classical Greek and Roman thinkers such as Democritus, Epicurus and Lucretins some centuries BC at the dawn of the scientific era, to the famous Nobel Prize Feynman conference 50 years ago ("There is plenty of room at the bottom"), phenomena at atomic scale have incessantly attracted the human spirit. However, to produce, touch, manipulate and create such atomistic-based systems has only been possible during the last 50 years as the appropriate technologies became available.

Books on micro- and nanosystems have already been written and continue to appear. They focus on the physics, chemical, technological and biological concepts, problems and applications. The dynamical modeling, estimation and feedback control are not classically addressed in the literature on miniaturization. However, these are innovative and efficient approaches to explore and improve; new small-scale systems could even be created.

The instruments for measuring and manipulating individual systems at molecular and atomic scale cannot be imagined without incorporating very precise estimation and feedback control concepts. On the other hand, to make such a dream feasible, control system methods have to adapt to unusual systems governed by different physics than the macroscopic systems. Phenomena which are usually neglected, such as thermal noise, become an important source of disturbances for nanosystems. Dust particles can represent obstacles when dealing with molecular positioning. The influence of the measuring process on the measured variable, referred to as back action, cannot be ignored if the measured signal is of the same order of magnitude as the measuring device noise.

This book is addressed to researchers, engineers and students interested in the domain of miniaturized systems and dynamical systems and information treatment at

this scale. The aim of this book is to present how concepts from dynamical control systems (modeling, estimation, observation, identification and feedback control) can be adapted and applied to the development of original very small-scale systems and to their human interfaces.

All the contributions have a model-based approach in common. The model is a set of dynamical system equations which, depending on its intended purpose, is either based on physics principles or is a black-box identified model or an energy (or potential field) based model. The model is then used for the design of the feedback control law, for estimation purposes (parameter identification or observer design) or for human interface design.

The applications presented in this book range from micro- and nanorobotics and biochips to near-field microscopy (Atomic Force and Scanning Tunneling Microscopes), nanosystems arrays, biochip cells and also human interfaces.

The book has three parts. The first part is dedicated to mini- and microsystems, with two applications of feedback control in micropositioning devices and microbeam dynamic shaping.

The second part is dedicated to nanoscale systems or phenomena. The fundamental instrument which we are concerned with is the microscope, which is either used to analyze or explore surfaces or to measure forces at an atomic scale. The core of the microscope is a cantilever with a sharp tip, in close proximity to the sample under analysis. Several chapters of the book treat different aspects related to the microscopy: force measurement at nanoscale is recast as an observer design, fast and precise nano-positioning is reached by feedback control design and cantilever arrays can be modeled and controlled using a non-standard approach. Another domain of interest is the field of biochips. A chapter is dedicated to the identification of a non-integer order model applied to such an electrochemical transduction/detection cell.

The third part of the book treats aspects of the interactions between the human and nanoworlds through haptic interfaces, telemanipulation and virtual reality.

Alina Voda
Grenoble
January 2010

PART I

Mini and Microsystems

Chapter 1

Modeling and Control of Stick-slip Micropositioning Devices

The principle of stick-slip motion is highly appreciated in the design of micropositioning devices. Indeed, this principle offers both a very high resolution and a high range of displacement for the devices. In fact, stick-slip motion is a step-by-step motion and two modes can therefore be used: the stepping mode (for coarse positioning) and the sub-step mode (for fine positioning). In this chapter, we present the modeling and control of micropositioning devices based on stick-slip motion principle. For each mode (sub-step and stepping), we describe the model and propose a control law in order to improve the performance of the devices. Experimental results validate and confirm the results in the theoretical section.

1.1. Introduction

In microassembly and micromanipulation tasks, i.e. assembly or manipulation of objects with submillimetric sizes, the manipulators should achieve a micrometric or submicrometric accuracy. To reach such a performance, the design of microrobots and micromanipulators is radically different from the design of classical robots. Instead of using hinges that may introduce imprecision, active materials are preferred. Piezoelectric materials are highly prized because of the high resolution and the short response time they can offer.

In addition to the high accuracy, a large range of motion is also important in microassembly/micromanipulation tasks. Indeed, the pick-and-place of small objects

---

Chapter written by Micky RAKOTONDRABE, Yassine HADDAB and Philippe LUTZ.

may require the transportation of the latter over a long distance. To execute tasks with high accuracy and over a high range of displacement, micropositioning devices and microrobots use embedded (micro)actuators. According to the type of microactuators used, there are different motion principles that can be used e.g. the stick-slip motion principle, the impact drive motion principle and the inch-worm motion principle. Each of these principles provides a step-by-step motion. The micropositioning device analyzed and experimented upon in this chapter is based on the stick-slip motion principle and uses piezoelectric microactuators.

Stick-slip micropositioning devices can work with two modes of motion: the coarse mode which is for long-distance positioning and the sub-step mode which is for fine positioning. This chapter presents the modeling and the control of the micropositioning device for both fine and coarse modes.

First we describe the micropositioning device. The modeling and control in fine mode are then analyzed. We then present the modeling in coarse mode, and end the chapter by describing control of the device in coarse mode.

1.2. General description of stick-slip micropositioning devices

1.2.1. *Principle*

Figure 1.1a explains the functioning of the stick-slip motion principle. In the figure, two microactuators are embedded onto a body to be moved. The two microactuators are made of a smart material. Here, we consider piezoelectric microactuators.

If we apply a ramp voltage to the microactuators, they slowly bend. As the bending acceleration is low, there is an adherence between the tips of the microactuators and the base (Figure 1.1b). If we reset the voltage, the bending of the legs is also abruptly halted. Because of the high acceleration, sliding occurs between their tips and the base. A displacement Δx of the body is therefore obtained (Figure 1.1c). Repeating the sequence using a sawtooth voltage signal makes the body perform a step-by-step motion. The corresponding motion principle is called stick-slip. The amplitude of a step is defined by the sawtooth voltage amplitude and the speed of the body is defined by both the amplitude and the frequency. The step value indicates the positioning resolution.

While the step-by-step motion corresponds to the coarse mode, it is also possible to work in sub-step mode. In this case, the rate of the applied voltage is limited so that the legs never slide (Figure 1.1d). In many cases, this mode is used when the error between the reference position and the present position of the device is less than one step. This mode is called fine mode.

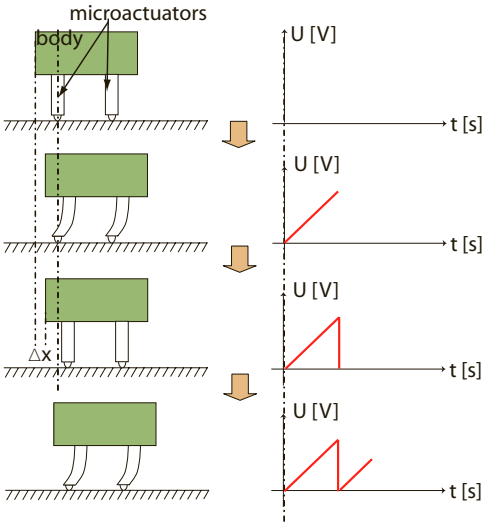

Figure 1.1. *Stick-slip principle: (a–c) stepping mode and (d) scanning mode*

1.2.2. *Experimental device*

The positioning device experimented upon in this paper, referred to as triangular RING (TRING) module, is depicted in Figure 1.2. It can perform a linear and an angular motion on the base (a glass tube) independently. Without loss of generality, our experiments are carried out only in linear motion. To move the TRING-module, six piezoelectric microactuators are embedded. Details of the design and development of the TRING-module are given in [RAK 06, RAK 09] while the piezoelectric microactuators are described in [BER 03].

To evaluate the step of the device, we apply a sawtooth signal to its microactuators. The measurements were carried out with an interferometer of $1.24\,\text{nm}$ resolution. Figure 1.3a depicts the resulting displacement at amplitude $150\,\text{V}$ and frequency $500\,\text{Hz}$. We note that the step is quasi-constant during the displacement. Figure 1.3b is a zoomed image of one step. The oscillations during the stick phase are caused by the dynamics of the microactuators and the mass of the TRING-module. The maximal step, obtained with $150\,\text{V}$, is about $200\,\text{nm}$. Decreasing the amplitude will decrease the value of the step and increase the resolution of the micropositioning device. As an example, with $U = 75\,\text{V}$ the step is approximatively $70\,\text{nm}$. However, the step efficiency is constant whatever the value of the amplitude. It is defined as the ratio of the gained step to the amplitude of the sawtooth voltage [DRI 03]:

$$\eta_{\text{step}} = \frac{\text{step}}{\Delta\text{amp}} \approx 0.7. \tag{1.1}$$

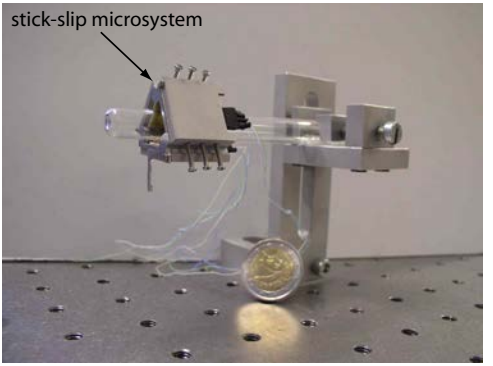

Figure 1.2. *A photograph of the TRING-module*

As introduced above, two modes of displacement are possible: the fine and the coarse modes. In the next sections, the fine mode of the TRING-module is first modeled and controlled. After that, we will detail the modeling and the control in coarse mode, all with linear motion.

1.3. Model of the sub-step mode

The sub-step modeling of a stick-slip micropositioning device is highly dependent upon the structure of microactuators. This in turn depends upon the required number of degrees of freedom and their kinematics, the structure of the device where they will be integrated and the structure of the base. For example, [FAT 95] and [BER 04] use two kinds of stick-slip microactuators to move the MICRON micropositioning device (5-dof) and the MINIMAN micropositioning device (3-dof). Despite this dependence of the model on the microactuator's structure, as long as the piezoelectric microactuator is operating linearly, the sub-step model is still linear [RAK 09].

During the modeling of the sub-step mode, it is of interest to include the state of the friction between the microactuators and the base. For example, it is possible to control it to be lower than a certain value to ensure the stick mode. There are several models of friction according to the application [ARM 94], but the elastoplastic model [DUP 02] is best adapted to the sub-step modeling. The model of the sub-step mode is therefore linear and has an order at least equal to the order of the microactuator model.

1.3.1. *Assumptions*

During the modeling, the adhesion forces between the foot of the microactuators and the base are assumed to be insignificant relative to the preload charge. The

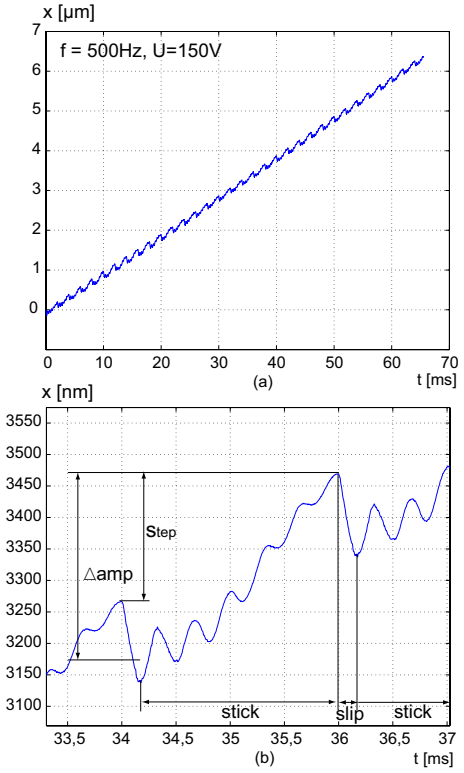

Figure 1.3. *Linear displacement measurement of the TRING-module using an interferometer: (a) a series of stick-slip motion obtained with $U = 150\,V$ and $f = 500\,Hz$ and (b) vibrations inside a step obtained with $U = 150\,V$ and $f = 60\,Hz$*

preload charge is the vertical force that maintains the device on the base. The base is considered to be rigid and we assume that no vibration affects it because we work in the stick mode. Indeed, during this mode, the tip of the microactuator and the base are fixed and shocks do not cause vibration.

To model the TRING micropositioning device, a physical approach has been applied [RAK 09]. While physical models of stick-slip devices strongly depend upon their structure and characteristics and on their microactuators, the structure of these models does not vary significantly. Assuming the piezoelectric microactuators work in the linear domain, the final model is linear. The order of the model is equal to the microactuator's model order added to the model order of the friction state. The sub-step modeling can be separated into two stages: the modeling of the microactuator (electromechanical part) and the inclusion of the friction model (mechanical part).

1.3.2. *Microactuator equation*

The different microactuators and the positioning device can be lumped into one microactuator supporting a body (Figure 1.4).

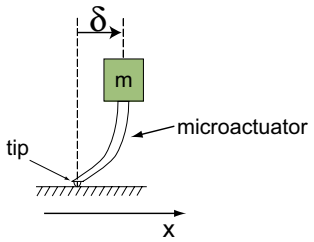

Figure 1.4. *Schematic of the microactuator*

If the microactuator works in a linear domain, a second-order lumped model is:

$$a_2\ddot{\delta} + a_1\dot{\delta} + \delta = d_p U + s_p F_{\text{piezo}} \tag{1.2}$$

where δ is the deflection of the microactuator, a_i are the parameters of the dynamic parts, d_p is the piezoelectric coefficient, s_p is the elastic coefficient and F_{piezo} is the external force applied to the microactuator. It may be derived from external disturbance (manipulation force, etc.) or internal stresses between the base and the microactuator.

1.3.3. *The elastoplastic friction model*

The elastoplastic friction model was proposed by Dupont *et al.* [DUP 02] and is well adapted for stick-slip micropositioning devices. Consider a block that moves along a base (Figure 1.5a). If the force F applied to the block is lower than a certain value, the block does not move. This corresponds to a stick phase. If we increase the force, the block starts sliding and the slip phase is obtained.

In the elastoplastic model, the contact between the block and the base are lumped in a medium asperity model (Figure 1.5b). Let G be the center of gravity of the block and x its motion. During the stick phase, the medium asperity bends. As there is no sliding ($\dot{w} = 0$), the motion of the block corresponds only to the deflection x_{asp} of the asperity: $x = x_{\text{asp}}$. This motion is elastic; when the force is removed, the deflection becomes null.

When the external force F exceeds a value corresponding to $x_{\text{asp}} = x_{\text{asp}}^{\text{ba}}$ (referred to as break-away), the tip of the asperity starts sliding and its displacement is given by

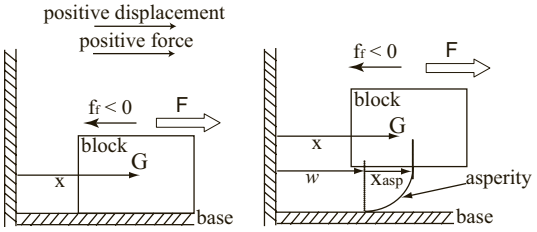

Figure 1.5. *(a) A block that moves along a base and (b) the contact between the block and the base can be approximated by a medium asperity*

w. While $\dot{w} \neq 0$, the deflection x_{asp} continues to vary. This phase is elastic because of x_{asp} but also plastic because of w.

If F is increased further, x_{asp} tends to a saturation called $x_{\text{asp}}^{\text{ss}}$ (steady state) and the speed $\dot{x}$ of the block is equal to $\dot{w} \neq 0$. This phase is called plastic because removing the force will not reset the block to its initial position.

The equations describing the elastoplastic model are:

$$\begin{aligned} x &= x_{\text{aps}} + w \\ f_f &= -N\left(\rho_0 x_{\text{asp}} + \rho_1 \dot{x}_{\text{asp}} + \rho_2 x\right) \\ \dot{x}_{\text{asp}} &= \dot{x}\left(1 - \alpha\left(x_{\text{asp}}, \dot{x}\right)\frac{x_{\text{asp}}}{x_{\text{asp}}^{\text{ss}}\left(\dot{x}\right)}\right) \end{aligned} \tag{1.3}$$

where N designates the normal force applied to the block, ρ_0 and ρ_2 are the Coulomb and the viscous parameters of the friction, respectively, ρ_1 provides damping for tangential compliance and $\alpha\left(x_{\text{asp}}, \dot{x}\right)$ is a function which determines the phase (stick or slip). Figure 1.6 provides an example of allure of α.

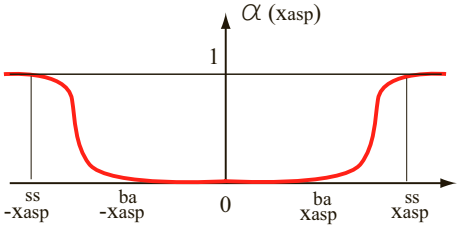

Figure 1.6. *An example of allure of* α

For stick-slip devices working in the sub-step mode, there is no sliding and so $\dot{w} = 0$. In addition, the coefficients ρ_1 and ρ_2 are negligible because the friction is dry (there is no lubricant). Assuming that the initial value is $w = 0$, the friction equations of stick-slip devices in the stick mode are:

$$\begin{aligned} f_f &= -N\rho_0 x_{\mathrm{asp}} \\ x &= x_{\mathrm{asp}} \\ \dot{x} &= \dot{x}_{\mathrm{asp}}. \end{aligned} \tag{1.4}$$

1.3.4. *The state equation*

To compute the model of the stick-slip micropositioning device in a stick mode, the deformation of the microactuator (equation (1.2)) and the friction model (equation (1.4)) are used. Figure 1.7 represents the same image as Figure 1.4 with the contact between the tip of the microactuator and the base enlarged. According to the figure, the displacement x_{sub} can be determined by combining the microactuator equation δ and the friction state x_{asp} using dynamic laws [RAK 09].

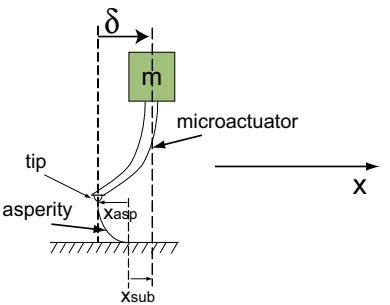

Figure 1.7. *An example of allure of* α

The state equation of the TRING-module is therefore:

$$\frac{d}{dt}\begin{bmatrix} \delta \\ \dot{\delta} \\ x_{\mathrm{asp}} \\ \dot{x}_{\mathrm{asp}} \end{bmatrix} = \begin{bmatrix} 0 & 1 & 0 & 0 \\ A_{21} & A_{22} & A_{23} & 0 \\ 0 & 0 & 0 & 1 \\ A_{41} & A_{42} & A_{43} & 0 \end{bmatrix} \begin{bmatrix} \delta \\ \dot{\delta} \\ x_{\mathrm{asp}} \\ \dot{x}_{\mathrm{asp}} \end{bmatrix} + \begin{bmatrix} 0 \\ B_2 \\ 0 \\ B_4 \end{bmatrix} U \tag{1.5}$$

where the state vector is composed of:

– the states of the electromechanical part: the deflection δ of the piezoelectric microactuator and the corresponding derivative $\dot{\delta}$; and

– the states of the friction part: the deflection of a medium asperity $x_{\rm asp}$ and the corresponding derivative $\dot{x}_{\rm asp}$.

The following values have been identified and validated for the considered system [RAK 09]:

$$\begin{aligned} A_{21} &= -1,023,243,521 \\ A_{22} &= -204,649 \\ A_{23} &= 44,183,761,041 \\ A_{41} &= 1,021,647,707 \\ A_{42} &= 204,330 \\ A_{43} &= -1,624,646,063,889 \end{aligned} \tag{1.6}$$

and

$$\begin{aligned} B_2 &= 0.969 \\ B_4 &= -0.9674 \end{aligned} \tag{1.7}$$

1.3.5. *The output equation*

The output equation is defined as

$$\begin{bmatrix} T \\ x_{\rm sub} \end{bmatrix} = \begin{bmatrix} C_{11} & C_{12} & C_{13} & 0 \\ 1 & 0 & 1 & 0 \end{bmatrix} \begin{bmatrix} \delta \\ \dot{\delta} \\ x_{\rm asp} \\ \dot{x}_{\rm asp} \end{bmatrix} + \begin{bmatrix} D_1 \\ 0 \end{bmatrix} U \tag{1.8}$$

where T is the friction and $x_{\rm sub}$ is the displacement of the mass m during the stick mode. $x_{\rm sub}$ corresponds to the fine position of the TRING device. The different parameters are defined:

$$\begin{aligned} C_{11} &= -1,596 \\ C_{12} &= -0.32 \\ C_{13} &= -1,580,462,303 \\ D_1 &= -1.5 \times 10^{-6}. \end{aligned} \tag{1.9}$$

1.3.6. *Experimental and simulation curves*

In the considered application, we are interested in the control of the position. We therefore only consider the output x_{sub}. From the previous state and output equations, we derive the transfer function relating the applied voltage and x_{sub}:

$$G_{x_{\mathrm{sub}}U} = \frac{x_{\mathrm{sub}}(s)}{U(s)} = \frac{1.5 \times 10^{-3}\left(s^2 + 1.01 \times 10^{15}\right)}{\left(s + 1.94 \times 10^{5}\right)\left(s + 5133\right)\left(s^2 + 5735s + 1.63 \times 10^{12}\right)} \tag{1.10}$$

where s is the Laplace variable.

To compare the computed model $G_{x_{\mathrm{sub}}U}$ and the real system, a harmonic analysis is performed by applying a sine input voltage to the TRING-module. The chosen amplitude of the sine voltage is 75 V instead of 150 V. Indeed, with a high amplitude the minimum frequency from which the drift (and then the sliding mode) starts is low. In the example of Figure 1.8, a frequency of 2250 Hz leads to a drift when the amplitude is 150 V while a frequency of 5000 Hz does not when amplitude is 75 V. The higher the amplitude, the higher the acceleration is and the higher the risk of sliding (drift). When the TRING-module slides, the sub-step model is no longer valuable.

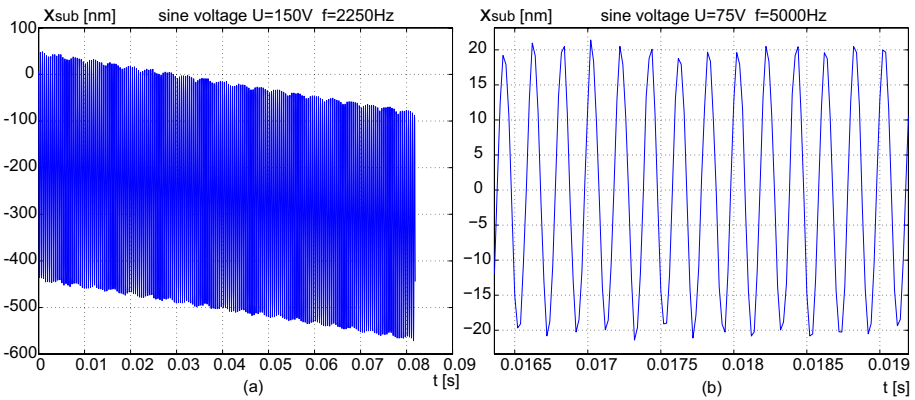

Figure 1.8. *Harmonic experiment: (a) outbreak of a drift of the TRING positioning system (sliding mode) and (b) stick mode*

Figure 1.9 depicts the magnitude of the simulation (equation (1.10)) and the experimental result. It shows that the structure of the model and the identified parameters correspond well.

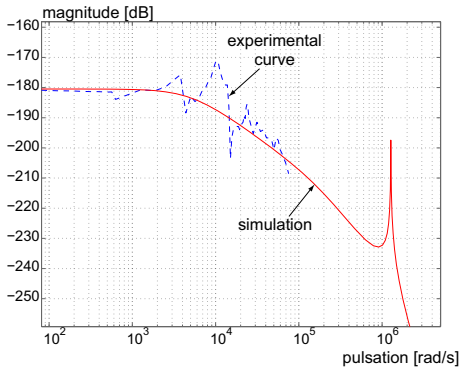

Figure 1.9. *Comparison of the simulation of the developed model and the experimental results*

1.4. PI control of the sub-step mode

The aim of the sub-step control is to improve the performance of the TRING-module during a highly accurate task and to eliminate disturbances (e.g. manipulation force, adhesion forces and environmental disturbances such as temperature). Indeed, when positioning a microcomponent such as fixing a microlens at the tip of an optical fiber [GAR 00], the manipulation force can disturb the positioning task and modify its accuracy. In addition, the numerical values of the model parameters may contain uncertainty. We therefore present here the closed-loop control of the fine mode to introduce high stability margins.

The sub-step functioning requires that the derivative dU/dt of the voltage should be inferior to a maximum slope $\dot{U}_{\max}$. To ensure this, we introduce a rate limiter in the controller scheme as depicted in Figure 1.10.

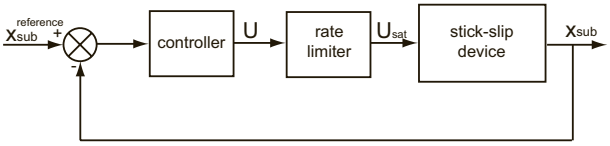

Figure 1.10. *Structure of the closed-loop system*

To ensure a null static error, we choose a proportional-integral (PI) controller. The parameters of the controller are computed to ensure a phase margin of $60°$, required for stability in residual phase uncertainty.

First, we trace the Black–Nichols diagram of the open-loop system $G_{x_{\text{sub}}U}$, as depicted in Figure 1.11.

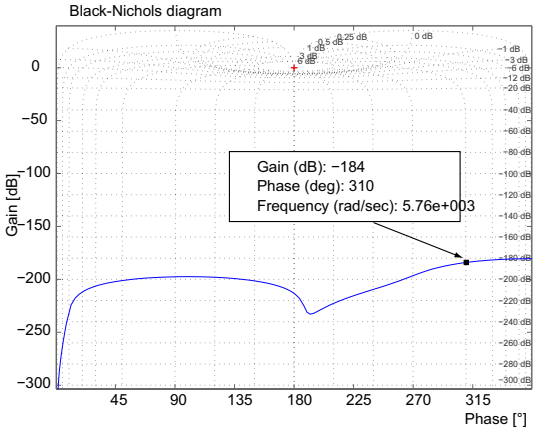

Figure 1.11. *Black–Nichols diagram of* $G_{x_{\text{sub}}U}$

Let

$$K_{\text{PI}} = K_p \times \left(1 + K_i \times \frac{1}{s}\right)$$

be the transfer function of the controller, where K_p and $K_i = 1/T_i$ are the proportional and the integrator gains, respectively. The 60° of phase margin is obtained if the new open-loop transfer function $K_{\text{PI}} \times G_{xU}$ has a Black–Nichols diagram which cuts the 0 dB horizontal axis at 240°. This can be obtained by computing a corrector K_{PI} that adjusts the data depicted in Figure 1.11 to that required. Using the computation method presented in [BOU 06], we find:

$$\begin{aligned} K_p &= 383,749,529 \\ K_i &= 7,940. \end{aligned} \tag{1.11}$$

The controller has been implemented following that depicted in Figure 1.10. The reference displacement is a step input signal $x_{\text{sub}}^{\text{ref}} = 100\,\text{nm}$. Figure 1.12a shows the experimental response of the TRING-module and the quasi-instantaneous response of the closed-loop system. The accuracy is about $\pm 5\,\text{nm}$ and the vibrations are due to the high sensitivity of the measurement to the environment. Such performances are of great interest in micromanipulation/microassembly.

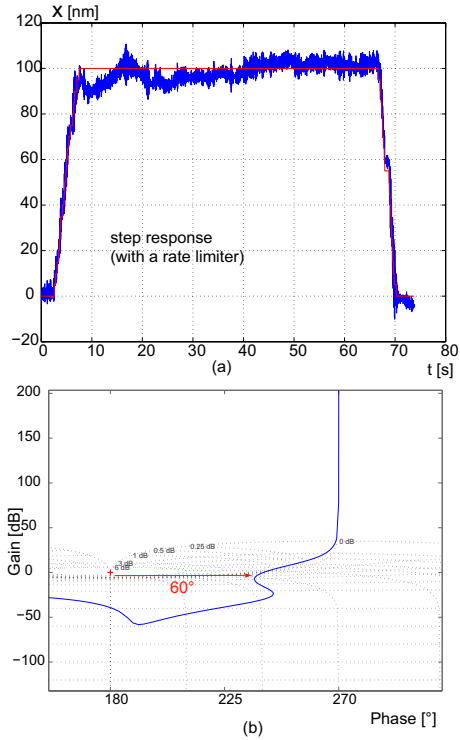

Figure 1.12. *Results of the PI control of the TRING-module in sub-step functioning*

Figure 1.12b shows the Black–Nichols diagram of the closed-loop system and indicates the margin phase. According to the figure, the margin gain is 50 dB. These robustness margins are sufficient to ensure the stability of the closed-loop system regarding the uncertainty of the parameters and of the structure of the developed model. Finally, the closed-loop control ensures these performances when external disturbances occur during the micromanipulation/microassembly tasks. A disturbance may be of an environmental type (e.g. temperature variation) or a manipulation type (e.g. manipulation force).

1.5. Modeling the coarse mode

When scanning over a large distance (e.g. pick-and-place tasks in microassembly), the micropositioning device should work in coarse mode. The applied voltage is no longer limited in slope as for the fine mode, but has a sawtooth form. The resulting displacement is a succession of steps. This section, which follows that of [BOU 06],

discusses the modeling and control of the coarse mode. The presented results are applicable to stepping systems.

1.5.1. *The model*

First, let us study one step. For that, we first apply a ramp input voltage up to U. If the slope of the ramp is weak, there is no sliding between the tip of the microactuators and the base. Using the model in the stick mode, the displacement of the device is defined:

$$x_{\text{sub}}(s) = G_{x_{\text{sub}}U}(s) \times U(s). \tag{1.12}$$

To obtain a step, the voltage is quickly reduced to zero. The resulting step x_{step} is smaller than the amplitude x_{sub} that corresponds to the last value of U (Figure 1.13a). We denote this amplitude x_{sub}^{U}. We then have:

$$x_{\text{step}} = x_{\text{sub}}^{U} - \Delta_{\text{back}}. \tag{1.13}$$

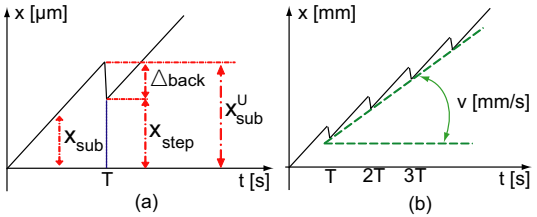

Figure 1.13. *(a) Motion of a stick-slip system and (b) speed approximation*

If we assume that backlash Δ_{back} is dynamically linear relative to the amplitude U, the step can be written as:

$$x_{\text{step}}(s) = G_{\text{step}}(s) \times U(s) \tag{1.14}$$

where G_{step} is a linear transfer function. When the sequence is repeated with a frequency $f = 1/T$, i.e. a sawtooth signal, the micropositioning device works in the stepping mode (coarse mode). During this mode, each transient part inside a step is no longer important. Instead, we are interested in the speed performance of the device over a large distance. To compute the speed, we consider the final value of a step:

$$x_{\text{step}} = \alpha \times U \tag{1.15}$$

where $\alpha > 0$ is the static gain of G_{step}.

From Figure 1.13b and equation (1.15), we easily deduce the speed:

$$v = \frac{x_{\text{step}}}{T} = x_{\text{step}} \times f. \tag{1.16}$$

The speed is therefore bilinear in relation to the amplitude U and the frequency f of the sawtooth input voltage:

$$v = \alpha f U. \tag{1.17}$$

However, the experiments show that there is a deadzone in the amplitude inside which the speed is null. Indeed, if the amplitude U is below a certain value U_0, the micropositioning system does not move in the stepping mode but only moves back and forth in the stick mode. To take into account this threshold, equation (1.15) is slightly modified and the final model becomes:

$$\begin{cases} v = 0 & \text{if} \quad |U| \leq U_0 \\ v = \alpha f \left(U - \text{sgn}(U) U_0\right) & \text{if} \quad |U| > U_0. \end{cases} \tag{1.18}$$

1.5.2. *Experimental results*

The identification on the TRING-module gives $\alpha = 15.65 \times 10^{-7} \text{mm V}^{-1}$ and $U_0 = 35\,\text{V}$. Figure 1.14 summarizes the speed performances of the micropositioning system: simulation of the model using equation (1.18) and experimental result. During the experiments, the amplitude U is limited to $\pm 150\,\text{V}$ in order to avoid the destruction of the piezoelectric microactutors. Figure 1.14a depicts the speed versus amplitude for three different frequencies. It shows that the experimental results fit the model simulation well. Figure 1.14b depicts the speed versus frequency. In this, the experimental results and the simulation curve correspond up to $f \approx 10\,\text{kHz}$; above this frequency there are saturations and fluctuations.

1.5.3. *Remarks*

To obtain equation (1.14), we made the assumption that the backlash Δback was linear relative to the amplitude U, such that in the static mode we have $\Delta\text{back} = K_{\text{back}} U$ where K_{back} is the static gain of the backlash. In fact, the backlash is pseudo-linear relative to U because K_{back} is dependent upon U.

Let $x_{\text{sub}}^U = G_{x_{\text{sub}}U}(0)\, U$ be the static value of x_{sub} in the sub-step mode obtained using equation (1.12) and corresponding to an input U, where $G_{x_{\text{sub}}U}(0)$ is a static gain. Substituting it into equation (1.13) and using equation (1.16), we have:

$$v = f\left(G_{x_{\text{sub}}U}(0)\, U - K_{\text{back}} U\right). \tag{1.19}$$

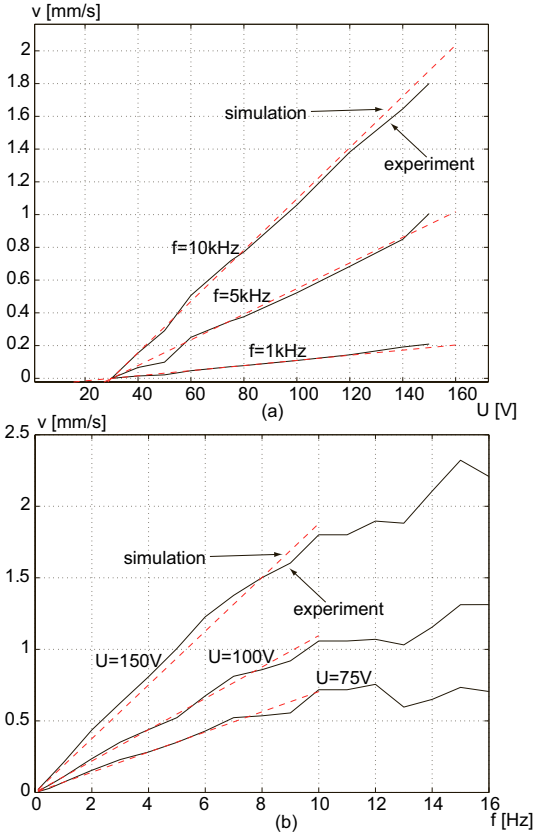

Figure 1.14. *Speed performances of the micropositioning system (experimental results in solid lines and simulation of equation (1.18) in dashed lines): (a) speed versus the amplitude U and (b) speed versus the frequency f*

Comparing equation (1.19) and the second equation of equation (1.18), we demonstrate the pseudo-linearity of the backlash in relation to U:

$$K_{\text{back}} = G_{x_{\text{sub}}U}(0) - \alpha\left(1 - \frac{U_0 \text{sgn}(U)}{U}\right). \tag{1.20}$$

1.6. Voltage/frequency (U/f) proportional control of the coarse mode

The micropositioning device working in coarse mode is a two-inputs-one-output system. The input variables are the frequency and the amplitude of the sawtooth voltage while the output is the displacement.

A stick-slip device is a type of stepping motor, and so stepping motor control techniques may be used. The easiest control of stepping motors is the open-loop counter technique. This consists of applying the number of steps necessary to reach a final position. In this, no sensor is necessary but the step value should be exactly known. In stick-slip micropositioning devices, such a technique is not very convenient. In fact, the friction varies along a displacement and the step is not very predictible. Closed-loop controllers are therefore preferred.

In closed-loop techniques, a natural control principle is the following basic algorithm:

$$\begin{aligned}&\text{WHILE } |x_c - x| \geq \text{step DO}\\&\text{apply 1 step}\\&\text{ENDWHILE}\end{aligned} \tag{1.21}$$

where x_c and x are the reference and the present positions of the stick-slip devices, respectively, and step is the value of one step. The resolution of the closed-loop system is equal to 1 step. If the accuracy of the sensor is lower than 1 step, a slight modification can be made:

$$\begin{aligned}&\text{WHILE } |x_c - x| \geq n \times \text{step DO}\\&\text{apply } n \times \text{step}\\&\text{ENDWHILE.}\end{aligned} \tag{1.22}$$

It is clear that for very precise positioning, the basic algorithm must be combined with a sub-step controller (such as the PI controller presented in the previous section). In that case, equation (1.21) is first activated during the coarse mode. When the error position $x_c - x$ is lower than the value of a step, the controller is switched into the sub-step mode.

In order to avoid the use of two triggered controllers for coarse mode and fine mode, Breguet and Clavel [BRE 98] propose a numerical controller where the frequency f of the sawtooth voltage is proportional to the error. In this, the position error is converted into a clock signal with frequency equal to that of the error. When the error becomes lower than a step, the frequency tends towards zero and the applied voltage is equivalent to that applied in the fine mode. Since the amplitude U is constant, the step is also constant and the positioning resolution is constant all along the displacement.